Journal of Process Control 19 (2009) 978–984

Contents lists available at ScienceDirect

Journal of Process Control

journal homepage: www.elsevier.com/locate/jprocont

An optimal feedforward control design for the set-point following of MIMO processes ☆

Stefano Piccagli, Antonio Visioli *

Dipartimento di Elettronica per l'Automazione, University of Brescia, Via Branze 38, I-25123 Brescia, Italy

ARTICLE INFO

Article history:
Received 19 June 2008
Received in revised form 22 December 2008
Accepted 23 December 2008

Keywords:
Multivariable processes
Feedforward control
Constrained control
Minimum-time transition
Multiobjective optimisation problem
PID control

ABSTRACT

In this paper we propose a new methodology for the design of a feedforward action for the improvement of the set-point following performance of feedback controlled square MIMO processes. In particular, by exploiting an analytical decoupling technique, the feedforward signals are determined in order to achieve predefined output transition times, by assuming that the transfer function matrix of the system consists of first order plus dead time transfer functions. An analytical expression of the feedforward signal is derived and this allows to solve easily a multiobjective optimisation problem in order to minimise the transition time of each output subject to constraints of the actuators. Simulation as well as experimental results demonstrate the effectiveness of the method.

1. Introduction

Proportional–Integral–Derivative (PID) controllers are undoubtedly the most widely adopted controllers in industry because of their capability to provide a satisfactory performance for a wide range of control tasks despite their relative ease of use. Actually, it is well known that the performance obtained by a PID controller much depends, in addition to the tuning of the PID parameters, to the appropriate implementation of those additional functionalities, such as anti-windup, set-point filtering, feedforward, and so on, that have to (or can) be added to the basic PID control law in order to deal with practical issues [1]. Methodologies for the effective design of these features are nowadays easier and easier to implement, due to the increase of computational power available in Distributed Control Systems (DCS) as well as in single-station controllers. In any case, in order to preserve the ease of use of the controller, these functionalities should be transparent to the user as much as possible or, alternatively, they have to be very intuitive.

In this context, a particular attention has been paid by researchers to the synthesis of a suitable feedforward control action in order to improve the set-point following performance. Different approaches have been devised. For example, a (linear) noncausal approach has been proposed in [2] for the continuous-time case and in [3] for the discrete-time case. In the context of causal techniques, with the aim of improving the classical linear feedforward controller design [4,5], a nonlinear feedforward action has been proposed in [6–8], where the constraints on the actuators are considered explicitly (note that the feedforward control action is applied directly to the actuator). In particular, in [8] a technique inspired by the bang–bang control strategy [9] is derived in order to obtain a user-defined process output transition time when a set-point change is required. The technique relies on assuming a first order plus dead time (FOPDT) model of the process and on applying a constant signal of a determined value for the predefined output transition time. The reference signal for the closed-loop system is determined at the same time by filtering appropriately the step reference signal.

However, in all these feedforward design approaches that have been proposed until now, only the single-input–single-output (SISO) case has been addressed, while many industrial processes are actually multivariable systems. Thus, in this paper we extend the method proposed in [8] to square multi-input–multi-output (MIMO) systems (with no RHP zeros). The analytical decoupling control strategy presented in [10] will be exploited for this purpose. Then, an analytical expression of the feedforward signal for each input is derived so that a multiobjective optimisation problem can be easily solved in order to minimise the transition time of each output subject to constraints of the actuators.

The paper is organised as follows. The feedforward design method is explained in Section 2. The optimisation problem is described in Section 3. Simulation results are presented in Section 4,

☆ This work has been supported partially by MIUR scientific research funds.
* Corresponding author. Tel.: +39 030 3715460; fax: +39 030 380014.
E-mail addresses: stefano.piccagli@ing.unibs.it (S. Piccagli), antonio.visioli@ing.unibs.it (A. Visioli).

0959-1524/$ - see front matter © 2009 Elsevier Ltd. All rights reserved.
doi:10.1016/j.jprocont.2008.12.010

while experimental results are shown in Section 5. Conclusions are drawn in Section 6.

2. Methodology

We consider a linear, time-invariant, continuous-time MIMO system whose matrix transfer function is:

$$\mathbf{P}(s) = \left[P_{ij}(s)\right] \; i,j = 1,\ldots,m, \tag{1}$$

where $P_{ij}(s)$ are assumed to be FOPDT transfer functions, namely,

$$P_{ij}(s) = \frac{K_{ij}}{T_{ij}s+1}e^{-L_{ij}s} \quad i,j = 1,\ldots,m. \tag{2}$$

The aim of the proposed methodology is to design a control scheme based on a feedback (PID) controller plus a feedforward term aiming at achieving, starting at time $t = 0$, a transition of each process output $\mathbf{y} = [y_1,\ldots,y_m]^T$ from the constant value $\mathbf{y}^0 = [y_1^0,\ldots,y_m^0]^T$ to the constant value $\mathbf{y}^1 = [y_1^1,\ldots,y_m^1]^T$ in predefined time intervals of duration $\boldsymbol{\tau} = [\tau_1,\ldots,\tau_m]^T$. Hereafter, for the sake of clarity and without loss of generality, null initial conditions will be assumed.

The overall control scheme is shown in Fig. 1 where $\mathbf{u_{ff}}$ is the feedforward action, $\mathbf{C}$ is the (decentralised) feedback controller, $\mathbf{F}$ filters each reference signal and the dashed part is not actually present in the control scheme but it is useful for the purpose of design. Indeed, $\mathbf{r}'$ is a fictitious command input and $\mathbf{D}$ is a decoupler to be determined by applying the analytical method presented in [10].

By assuming $\mathbf{r_f} = \mathbf{y}$, denote as $\mathbf{H}$ the closed-loop system transfer matrix from $\mathbf{r}'$ to $\mathbf{y}$, which can be determined as

$$\mathbf{H}(s) = \mathbf{P}(s)\mathbf{D}(s)(\mathbf{I} + \mathbf{P}(s)\mathbf{D}(s))^{-1}. \tag{3}$$

Ideally, $\mathbf{H}(s)$ should have a diagonal form, namely,

$$\mathbf{H}(s) = \begin{bmatrix} H_{11}(s) & 0 & \cdots & \cdots & 0 \\ 0 & H_{22}(s) & 0 & \cdots & 0 \\ & & & & \\ 0 & \ddots & \ddots & \ddots & 0 \\ 0 & \cdots & \cdots & 0 & H_{mm}(s) \end{bmatrix}. \tag{4}$$

Substituting (4) into (3) we obtain the decoupler expression

$$\mathbf{D}(s) = \mathbf{P}^{-1}(s)\left(\mathbf{H}^{-1}(s) - \mathbf{I}\right)^{-1} = \mathbf{W}(s)\mathrm{diag}\left[\frac{H_{ii}(s)}{1-H_{ii}(s)}\right]_{m\times m}, \tag{5}$$

where

$$\mathbf{W}(s) = \frac{\mathrm{adj}(\mathbf{P}(s))}{\det(\mathbf{P}(s))} \tag{6}$$

and $\mathrm{adj}(\mathbf{P}(s))$ is the adjoint of the process transfer matrix $\mathbf{P}(s)$. We can rewrite $\mathbf{W}(s)$ as

$$\mathbf{W}(s) = \left[G_{ij}(s)e^{\bar{L}_{ij}s}\right] \quad i,j = 1,\ldots,m, \tag{7}$$

where $\bar{L}_{ij}$ are suitable scalars so that $G_{ij}(s)$ has at least one polynomial term in the denominator that does not include any time delay. Then, a rational expression for $G_{ij}(s)$ is obtained by using the linear fractional Padé expansion [10].

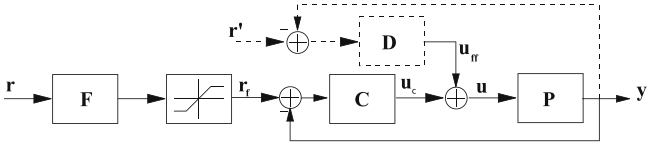

Fig. 1. The overall control scheme.

In particular, when the process has no RHP zeros (see Remark 2), if the diagonal elements of the decoupled system matrix are chosen as

$$H_{ii}(s) = \frac{e^{-\theta_i s}}{T_{ii}s+1} \quad i = 1,\ldots,m, \tag{8}$$

where

$$\theta_i = \max\{L_{i1},\ldots,L_{im}\} \quad i = 1,\ldots,m, \tag{9}$$

then, the resulting elements of the decoupler transfer matrix can be determined analytically as [10]

$$D_{ji}(s) = \frac{G_{ij}(s)e^{-(\theta_i - L_{ij})s}}{T_{ii}s+1}\frac{1}{1-\frac{e^{-\theta_i s}}{T_{ii}s+1}} \quad j,i = 1,\ldots,m. \tag{10}$$

Once the decoupler $\mathbf{D}$ has been designed, the feedforward action $\mathbf{u_{ff}}$ can be determined by applying the method described in [8] to the m SISO systems $H_{ii}(s), i = 1,\ldots,m$. In particular, $\mathbf{u_{ff}}$ results from the application of the command input $\mathbf{r}'$ that yields the desired output transition, namely, each command input $r_i', i = 1,\ldots,m$ is selected as

$$r_i'(t) = \begin{cases} \bar{r}_i' & \text{if} \quad t < \tau_i, \\ y_i^1 & \text{if} \quad t \geqslant \tau_i, \end{cases} \; i = 1,\ldots,m, \tag{11}$$

where

$$\bar{r}_i' = \frac{y_i^1}{1-e^{-\tau_i/T_{ii}}} \quad i = 1,\ldots,m. \tag{12}$$

It is worth stressing that if the process is described perfectly by the model (1) and (2), then, the process output is given by the application of the input (11) and (12) to the decoupled process (4). In particular, for $t \geqslant \tau_i + \theta_i$ the ith output is given by the difference of two step responses (where the second one is delayed by τ_i with respect to the first one), namely,

$$\begin{aligned} y_i(t) &= \frac{y_i^1}{1-e^{-\tau_i/T_{ii}}}\left(1-e^{-\frac{t-\theta_i}{T_{ii}}}\right) \\ &\quad + \left(y_i^1 - \frac{y_i^1}{1-e^{-\tau_i/T_{ii}}}\right)\left(1-e^{-\frac{t-\theta_i-\tau_i}{T_{ii}}}\right) \\ &= y_i^1. \end{aligned} \tag{13}$$

Thus, formally, we have that the nominal system output is

$$y_i(t) = \begin{cases} 0 & \text{if} \quad t \leqslant \theta_i, \\ \bar{r}_i'(1-\exp(-(t-\theta_i)/T_{ii})) & \text{if} \quad \theta_i < t < \theta_i + \tau_i, \\ y_i^1 & \text{if} \quad t \geqslant \theta_i + \tau_i, \end{cases} \; i = 1,\ldots,m. \tag{14}$$

Then, by taking into account that the closed-loop reference signal vector $\mathbf{r_f}$ has to be equal to the desired process output, each step reference signal r_i of amplitude y_i^1 has to be filtered by the system

$$F_{ii}(s) = \frac{\bar{r}_i'/y_i^1}{T_{ii}s+1}e^{-\theta_i s} \quad i = 1,\ldots,m \tag{15}$$

and then saturated at the level y_i^1. Thus, it is

$$\mathbf{F}(s) = \begin{bmatrix} \frac{\bar{r}_1'/y_1^1}{T_{11}s+1}e^{-\theta_1 s} & 0 & \cdots & \cdots & 0 \\ 0 & \frac{\bar{r}_2'/y_2^1}{T_{22}s+1}e^{-\theta_2 s} & 0 & \cdots & 0 \\ & & & & \\ 0 & \ddots & \ddots & \ddots & 0 \\ 0 & \cdots & \cdots & 0 & \frac{\bar{r}_m'/y_m^1}{T_{mm}s+1}e^{-\theta_m s} \end{bmatrix}. \tag{16}$$

Unavoidable model uncertainties are handled by a feedback action which can be provided by (decentralised) PID controllers that can be tuned by any conventional method [11,12].

Remark 1. It is worth stressing that feedback PID controllers have been considered because, as already mentioned, they are the most employed controllers in industry. However, the design methodology for the feedforward control design is independent of the structure of the feedback controllers and can be therefore applied with any feedback controllers.

Remark 2. While numerical procedures can be applied in general in order to verify that the process has no RHP zeros [10], the dual-locus diagram method [13] can be exploited in the relevant case $m = 2$. In particular, the transmission zeros of the system (1) and (2) are the solution of the following equation:

$$\frac{K_{11}}{T_{11}s+1}e^{-L_{11}s}\frac{K_{22}}{T_{22}s+1}e^{-L_{22}s} - \frac{K_{12}}{T_{12}s+1}e^{-L_{12}s}\frac{K_{21}}{T_{21}s+1}e^{-L_{21}s} = 0, \tag{17}$$

which can be rewritten as

$$e^{-\bar{L}s} = \phi(s), \tag{18}$$

where

$$\bar{L} = L_{11} + L_{22} - (L_{12} + L_{21}) \tag{19}$$

and

$$\phi(s) = \left(\frac{K_{12}K_{21}}{K_{11}K_{22}}\right)\frac{(T_{11}T_{22})s^2 + (T_{11}+T_{22})s + 1}{(T_{12}T_{21})s^2 + (T_{12}+T_{21})s + 1}. \tag{20}$$

Eq. (18) can be solved with the dual-locus diagram method, looking for the interceptions between the unit circle ($e^{-\bar{L}s}$) and the Nyquist curve of $\phi(s)$. The unit circle can be covered either clockwise or counterclockwise according to the sign of $\phi(s)$.

Remark 3. In general, the selection of the time constant for each diagonal element of the decoupled system matrix (8) is arbitrary. Here, the choice of using $T_{ii}, i = 1, \ldots, m$ (namely, the same time constants of the diagonal elements of the process transfer matrix), which is sensible from a practical point of view, is motivated by the fact that a simple optimisation problem is eventually posed (see Section 3). In any case, note again that the output transition times, which are the relevant parameters in order to satisfy the control requirements, can be selected arbitrarily.

Remark 4. It is worth stressing that, among the different decoupling strategies that have been proposed (see, for example, [14,15]), we selected that presented in [10] because it allows to obtain analytically a decoupled multivariable transfer function with FOPDT elements.

3. Multiobjective optimisation

From a practical point of view the user can define the transition times according to the control specifications and then the feedforward action can be determined by following the methodology explained in Section 2. Alternatively, the transition times can be minimised subject to the saturation constraints of the actuator, that is, subject to limits on the control variable $\mathbf{u}$. However, by taking into account that in the nominal case, the output $\mathbf{u}_c$ of the feedback controller is zero, the constraints can be equivalently posed to the feedforward vector signal $\mathbf{u_{ff}}$. This actually yields to the construction of a Pareto set of output transition times. Formally, the multiobjective optimisation problem (MOP) can be posed as follows:

$$\min_{\boldsymbol{\tau}\in\mathbb{R}_+^m} \boldsymbol{\tau} \tag{21}$$

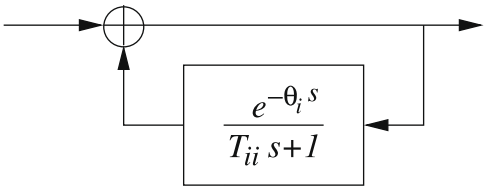

Fig. 2. Positive feedback loop $L(s)$.

subject to

$$u_{m,i} \leqslant \mathbf{u_{ff}}_i(t) \leqslant u_{M,i} \quad \forall t \geqslant 0 \quad i = 1, \ldots, m, \tag{22}$$

where $\mathbb{R}_+$ denotes the set of positive real numbers and the values $u_{m,i}$ $u_{M,i}, i = 1, \ldots, m$ are, respectively, the minimum and maximum given saturation limits of the actuators.

Let the feasible set of the MOP (21) and (22) be denoted as

$$\mathscr{F} := \{\boldsymbol{\tau} \in \mathbb{R}_+^m : u_{m,i} \leqslant \mathbf{u_{ff}}_i(t) \leqslant u_{M,i}\ \forall t \geqslant 0,\ i = 1, \ldots, m\}. \tag{23}$$

Denoting by $\partial\mathscr{F}$ the boundary of the feasible set $\mathscr{F}$ we have that the Pareto set that is the solution of the addressed MOP is

$$\mathscr{P} := \{\boldsymbol{\tau}^* \in \partial\mathscr{F} : \nexists \boldsymbol{\tau} \in \partial\mathscr{F} : \{\boldsymbol{\tau} \leqslant \boldsymbol{\tau}^* \text{ and } \exists \tau_i : \tau_i < \tau_i^*\}\}. \tag{24}$$

In order to solve the optimisation problem, it is useful to determine an analytical expression of the feedforward vector signal $\mathbf{u_{ff}}(t)$. An obstacle for this is represented by the positive feedback loop

$$L(s) := \frac{1}{1 - \frac{e^{-\theta_i s}}{T_{ii}s+1}} \tag{25}$$

in the elements of the decoupler transfer matrix $\mathbf{D}(s)$ (see (10)). However, it can be recognised that this feedback structure (see Fig. 2) is the same of the integral part of a PI controller in automatic reset configuration with the addition of a dead time [1]. Thus, a convenient way of approximating the transfer function (25) is to consider the following system:

$$\tilde{L}(s) := 1 + \frac{K_i}{s}e^{-\bar{\theta}_i s}, \tag{26}$$

where K_i and $\bar{\theta}_i$ can be determined by solving the following equations that impose, respectively, that the final value of the impulse and step responses are the same, namely:

$$\lim_{s\to 0} s\tilde{L}(s) = \lim_{s\to 0} sL(s) \tag{27}$$

and

$$\lim_{s\to 0} \tilde{L}(s) = \lim_{s\to 0} L(s). \tag{28}$$

This yields to:

$$K_i = \frac{1}{T_{ii} + \theta_i} \tag{29}$$

and

$$\bar{\theta}_i = \frac{1}{2}\frac{\theta_i(2T_{ii} + \theta_i)}{T_{ii} + \theta_i}. \tag{30}$$

An example of the accuracy of the step response approximation is given in Fig. 3, where the values $T_{ii} = 10$ and $\theta_i = 2$ have been selected (note that it is $K_i = 0.083$ and $\bar{\theta}_i = 1.83$). Once $L(s)$ is approximated by $\tilde{L}(s)$, $\mathbf{u_{ff}}(t)$ can be determined as

$$\mathbf{u_{ff}}(t) = \mathscr{L}^{-1}\{\mathbf{D}(s)[\mathbf{R}'(s) - \mathbf{Y}(s)]\}, \tag{31}$$

where $\mathscr{L}^{-1}$ is the inverse Laplace transform operator, $\mathbf{R}'(s)$ is the Laplace transform of the command input vector $\mathbf{r}'(t)$ (see (11)) and $\mathbf{Y}(s)$ is the Laplace transform of the nominal output vector $\mathbf{y}(t)$

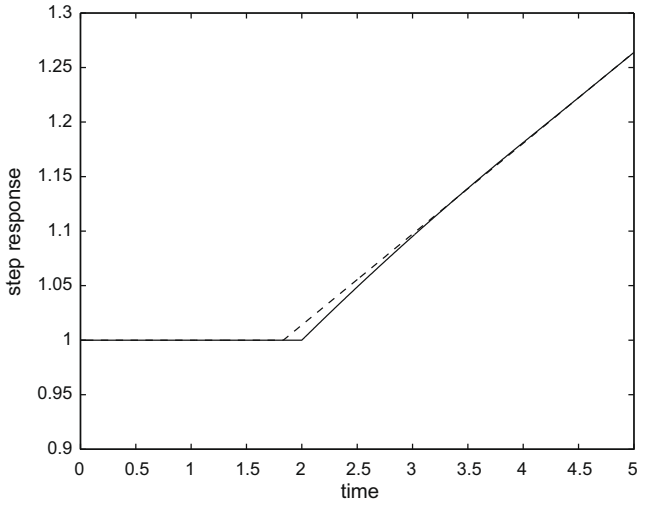

Fig. 3. Step response of $L(s)$ (dashed line) and $\tilde{L}(s)$ (solid line) for $T_{ii} = 10$ and $\theta_i = 2$.

(see (14)). The Laplace transform of elements of the command input vector can be derived from (11) as

$$R_i'(s) = \frac{\bar{r}_i'}{s} - \frac{\bar{r}_i' - y_i^1}{s} e^{-\tau_i s} \quad i = 1, \ldots, m, \tag{32}$$

while the Laplace transform of the elements of the nominal output vector can be derived from (14) as

$$Y_i(s) = \frac{y_i^1}{T_{ii}(1 - e^{-\tau_i/T_{ii}})} \frac{1}{s + 1/T_{ii}} e^{-\theta_i s} - \frac{y_i^1 e^{-\tau_i/T_{ii}}}{T_{ii}(1 - e^{-\tau_i/T_{ii}})} \times \frac{1}{s + 1/T_{ii}} e^{-(\theta_i + \tau_i)s} \quad i = 1, \ldots, m. \tag{33}$$

Once the (approximated) analytical expression of the feedforward action is available, the Pareto set of the multiobjective optimisation problem can be determined quite straightforwardly by adopting a standard multiobjective optimization procedure such as the ε-constraint method [16]. Note that the set is not convex in general (see Section 4).

Remark 5. From a practical point of view, in order to address the robustness issue, it is worth to consider constraints in (22) that are slightly smaller than the actual physical limits of the actuators. In fact, the actuator should be also capable to provide the control action determined by the feedback PID controllers due to the unavoidable model uncertainties.

Remark 6. It is worth stressing that, once the output transition times have been selected, the feedforward control law can be implemented either by applying the analytical expression of $\mathbf{u_{ff}}(t)$ or by implementing explicitly the dashed part of the control scheme in Fig. 1 (for example in a Distributed Control System) and by applying the command signal vector $\mathbf{r}'(t)$.

4. Simulation results

In order to show the effectiveness of the proposed methodology, the Shell Heavy Oil Fractionator benchmark problem [17] has been considered as a first example. This process is described by the following transfer function (where inputs are the top and side draws while outputs are top and side end points of a distillation column) with $m = 2$:

$$\mathbf{P}(s) = \begin{bmatrix} \frac{4.05}{50s+1} e^{-27s} & \frac{1.77}{60s+1} e^{-28s} \\ \frac{5.39}{50s+1} e^{-28s} & \frac{5.72}{60s+1} e^{-14s} \end{bmatrix}. \tag{34}$$

The decentralised feedback controllers have been selected of PI type, namely:

$$\mathbf{C}(s) = \begin{bmatrix} K_{p1}\left(1 + \frac{1}{T_{i1}s}\right) & 0 \\ 0 & K_{p2}\left(1 + \frac{1}{T_{i2}s}\right) \end{bmatrix}. \tag{35}$$

They have been tuned by applying the BLT method [18]. The resulting parameters are: $K_{p1} = 0.27$, $T_{i1} = 112.5, K_{p2} = 0.39, T_{i2} = 63.9$. The limits on the control variable have been posed as $u_{m1} = u_{m2} = -0.6$ and $u_{M1} = u_{M2} = 0.6$. The result of the MOP for $\mathbf{y}^1 = [1\,1]$, where a discretisation of 0.2 has been selected for the transition time τ_1, is shown in Fig. 4. It is clear that for $\tau_1 < 19$ there is no value of τ_2 for which the desired transition is obtained without exceeding the limits posed on u_1 and u_2. The process outputs and the control variables obtained by choosing $\tau_1^* = 22.2$ and $\tau_2^* = 58.5$ are shown in Fig. 5. It is worth noting that the control variable $\mathbf{u}$ is determined only by the feedforward action $\mathbf{u_{ff}}$, namely, the contribution of the feedback PI controllers is negligible. The results obtained if the feedforward action is not employed, that is, by using only the PI controllers are plotted for comparison.

The results obtained for the cases $\mathbf{y}^1 = [1\,0]$ ($\tau_1^* = 70$) and $\mathbf{y}^1 = [0\,1]$ ($\tau_2^* = 40$) are plotted in Figs. 6 and 7, respectively. The system is virtually decoupled as expected.

It appears that the process variables are as desired and the control variables do not exceed their limits.

As a second illustrative example, a higher order system [19] with $m = 2$ has been considered:

$$\mathbf{P}(s) = \begin{bmatrix} \frac{-0.1153(10s+1)}{(4s+1)^3} e^{-0.1s} & \frac{0.2429}{(33s+1)^2} e^{-2s} \\ \frac{-0.0887}{(43s+1)(22s+1)} e^{-12.6s} & \frac{0.2429}{(44s+1)(20s+1)} e^{-0.17s} \end{bmatrix}. \tag{36}$$

The FOPDT transfer functions have been identified through the step-test method described in [20], yielding:

$$\mathbf{P}(s) = \begin{bmatrix} \frac{-0.1155}{3.5s+1} e^{-0.66s} & \frac{0.243}{57.6s+1} e^{-12.7s} \\ \frac{-0.0887}{63.2s+1} e^{-17.6s} & \frac{0.243}{55.5s+1} e^{-10.2s} \end{bmatrix}. \tag{37}$$

Decentralised PI controllers have been tuned by applying again the BLT method [18] that yields the following parameters: $K_{p1} = -16.6, T_{i1} = 20.75, K_{p2} = 70.6, T_{i2} = 80.23$. The limits on the control variable have been posed as $u_{m1} = -7, u_{m2} = -11, u_{M1} = 7$, and $u_{M2} = 11$. The result of the MOP for $\mathbf{y}^1 = [1\,1]$, where a discretisation of 0.2 has been selected for the transition time τ_1, is shown

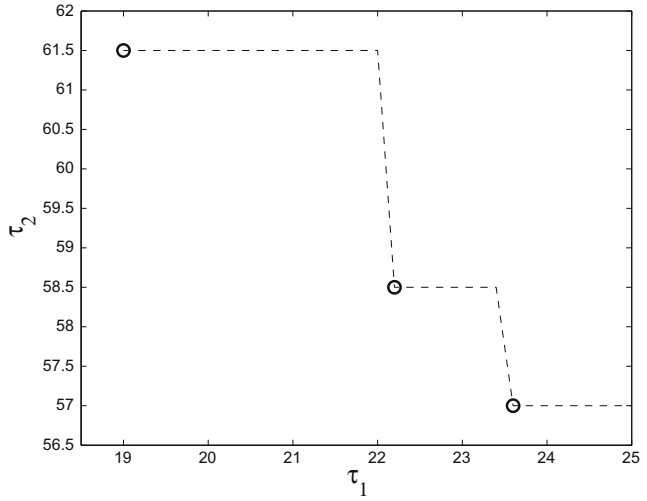

Fig. 4. Results of the MOP for the first example. Dashed line: boundary $\partial\mathscr{F}$ of the feasible set. Circles: Pareto set $\mathscr{P}$.

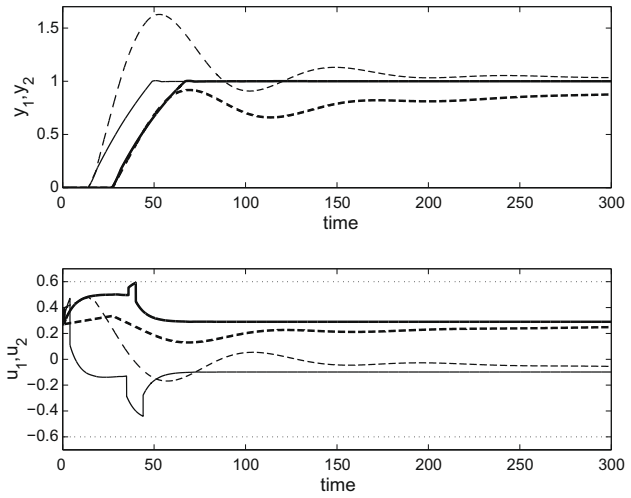

Fig. 5. Output of the system (34) when $\mathbf{y}^1 = [1\,1]$. Solid thick line: y_1 and u_1 with feedforward action. Solid thin line: y_2 and u_2 with feedforward action. Dashed thick line: y_1 and u_1 without feedforward action. Dashed thin line: y_2 and u_2 without feedforward action.

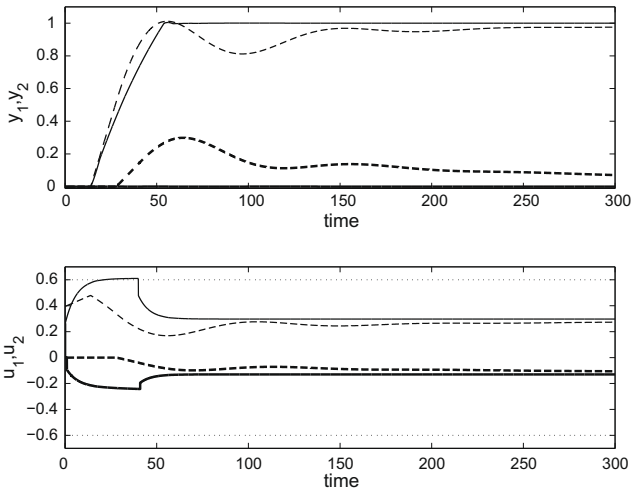

Fig. 7. Output of the system (34) when $\mathbf{y}^1 = [0\,1]$. Solid thick line: y_1 and u_1 with feedforward action. Solid thin line: y_2 and u_2 with feedforward action. Dashed thick line: y_1 and u_1 without feedforward action. Dashed thin line: y_2 and u_2 without feedforward action.

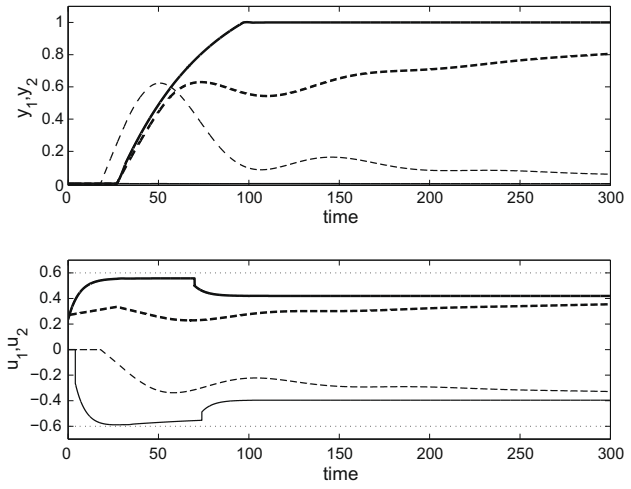

Fig. 6. Output of the system (34) when $\mathbf{y}^1 = [1\,0]$. Solid thick line: y_1 and u_1 with feedforward action. Solid thin line: y_2 and u_2 with feedforward action. Dashed thick line: y_1 and u_1 without feedforward action. Dashed thin line: y_2 and u_2 without feedforward action.

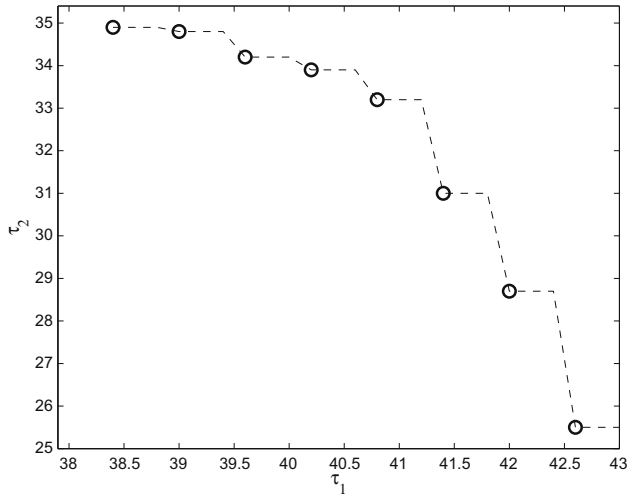

Fig. 8. Results of the MOP for the second example. Dashed line: boundary $\partial\mathscr{F}$ of the feasible set. Circles: Pareto set $\mathscr{P}$.

in Fig. 8. The process outputs and the control variables obtained by choosing $\tau_1^* = 39.6$ and $\tau_2^* = 34.2$ are shown in Fig. 9. The results obtained by using only the feedback PI controllers are plotted again for comparison. It appears that the devised technique is effective also in the presence of unstructured uncertainties. Note that the use of the feedforward action allows to attain the actuator saturation limits for very small time intervals, thus preserving the linear behaviour of the control system.

5. Experimental results

In order to prove the effectiveness of the devised technique in practical applications, a laboratory experimental setup (made by KentRidge Instruments) has been employed (see a sketch of the process in Fig. 10). Specifically, the apparatus consists of two coupled small perspex tower-type tanks (whose area is 40 cm^2). Water is pumped into the top of each tank by two independent pumps whose speeds are set by DC voltages (the manipulated variables), in the range 0–5 V, through a PWM circuits. Each tank is fitted with an outlet at the base in order for the water to return to a reservoir. Then, a leakage between the two tanks is allowed in order to obtain coupling between them. Thus, the apparatus is a two-inputs–two-outputs system in which a level control is implemented by means of a PC-based controller. For each tank, the measure of the level of the water is given by a capacitive-type probe that provides an output signal between 0 (empty tank) and 5 V (full tank). For the sake of simplicity, the level variables will be expressed in Volts hereafter. Note that the system has a nonlinear dynamics, because the flow rate out of a tank depends on the square root of its level.

The selected control task requires a transition from $\mathbf{y}^0 = [2.2\ 2.2]$ V to $\mathbf{y}^1 = [3.2\ 3.2]$ V. The FOPDT transfer functions have been identified through the step-test method described in [20], yielding:

$$\mathbf{P}(s) = \begin{bmatrix} \frac{1.12}{30.37s+1}e^{-s} & \frac{0.84}{40.95s+1}e^{-2s} \\ \frac{0.81}{18.76s+1}e^{-4s} & \frac{0.93}{21.25s+1}e^{-s} \end{bmatrix}. \quad (38)$$

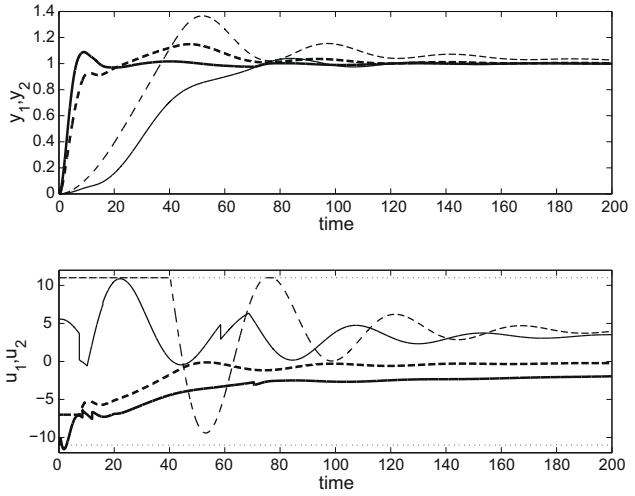

Fig. 9. Output of the system (36) when $\mathbf{y}^1 = [1\,1]$. Solid thick line: y_1 and u_1 with feedforward action. Solid thin line: y_2 and u_2 with feedforward action. Dashed thick line: y_1 and u_1 without feedforward action. Dashed thin line: y_2 and u_2 without feedforward action.

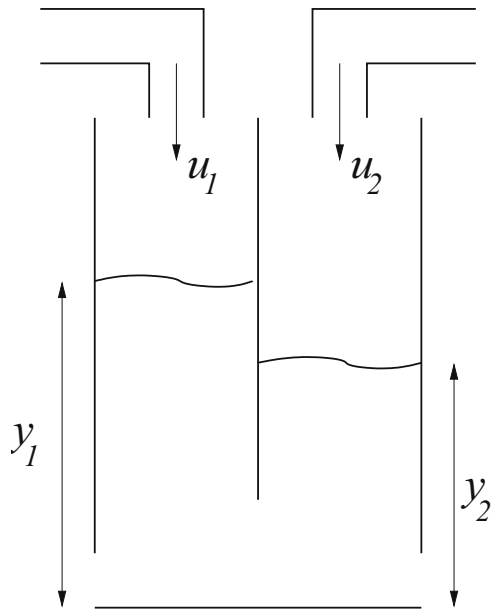

Fig. 10. The experimental setup for the level control experiment.

The following values of parameters for the decentralised PI controllers were computed using BLT algorithm: $K_{p1} = 5.42, T_{i1} = 10.04, K_{p2} = 4.60, T_{i2} = 10$. By taking into account the physical limits of the actuators and the effect of the uncertainties, the limits on the control variable for the MOP have been posed as $u_{m1} = u_{m2} = 0$ and $u_{M1} = u_{M2} = 4.6$. The resulting Pareto set $\mathscr{P}$, together with the boundary $\partial\mathscr{F}$ of the feasible set is shown in Fig. 11. The process outputs and the control variables obtained by choosing $\tau_1^* = 25.36$ and $\tau_2^* = 17.25$ are shown in Fig. 12. The results obtained by using only the feedback PI controllers are plotted in Fig. 13. It appears that the feedforward action allows to improve the set-point following performance with respect to the decentralised PI control, especially by avoiding the detrimental effects of the saturations of the actuators.

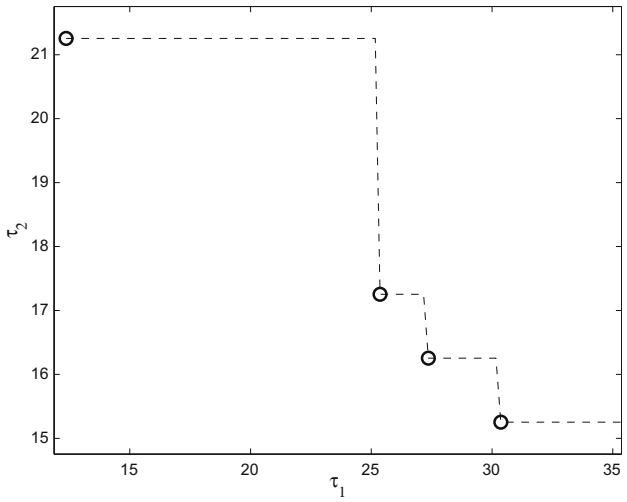

Fig. 11. Results of the MOP for the coupled tank apparatus. Dashed line: boundary $\partial\mathscr{F}$ of the feasible set. Circles: Pareto set $\mathscr{P}$.

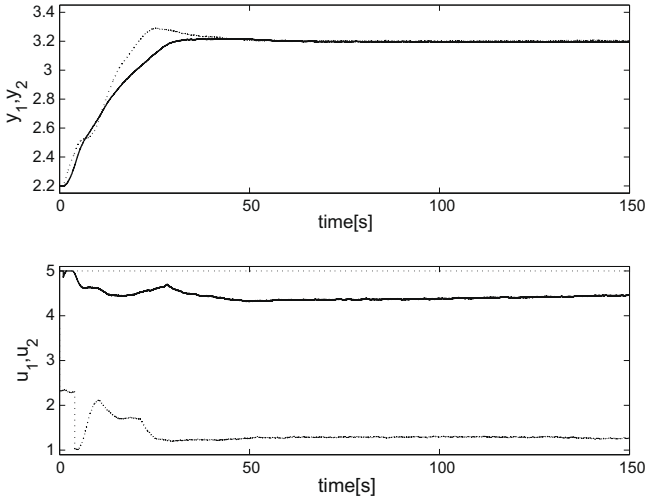

Fig. 12. Output of the coupled tank apparatus. Solid line: y_1 and u_1 with feedforward action. Dashed line: y_2 and u_2 with feedforward action.

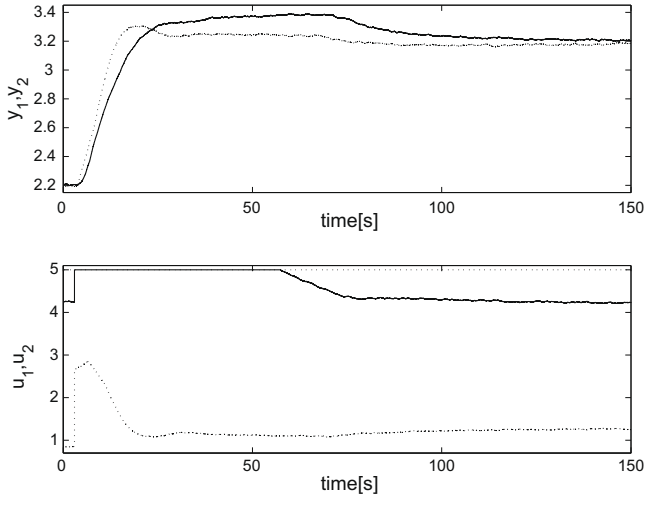

Fig. 13. Output of the coupled tank apparatus. Solid line: y_1 and u_1 without feedforward action. Dashed line: y_2 and u_2 without feedforward action.

6. Conclusions

In this paper we have proposed a new methodology for the design of a nonlinear feedforward control action for the set-point following control task to be applied to a MIMO process. A key role in the method is played by an analytical decoupling technique which allows to solve a multiobjective optimisation problem to minimise the output transition times subject to limits of the actuator. Practical considerations have been highlighted and simulation as well as experimental results have demonstrated the effectiveness of the methodology which appears to be suitable to implement in standard Distributed Control Systems.

References

[1] A. Visioli, Practical PID Control, Springer, London, UK, 2006.
[2] A. Piazzi, A. Visioli, A noncausal approach for PID control, Journal of Process Control 16 (8) (2006) 831–843.
[3] A. Visioli, A. Piazzi, Improving set-point following performance of industrial controllers with a fast dynamic inversion algorithm, Industrial and Engineering Chemistry Research 42 (2003) 1357–1362.
[4] K.J. Åström, T. Hägglund, Advanced PID Control, ISA Press, Research Triangle Park, NC, 2006.
[5] B.C. Kuo, Automatic Control Systems, Prentice Hall, Englewood Cliffs, NJ, 1995.
[6] A. Wallen, Tools for Autonomous Process Control, Ph.D. Thesis, Lund Institute of Technology, 2000.
[7] A. Wallen, K.J. Åström, Pulse-step control, Preprints of the 15th IFAC World Congress on Automatic Control, Barcelona, Spain, 2002.
[8] A. Visioli, A new design for a PID plus feedforward controller, Journal of Process Control 14 (4) (2004) 455–461.
[9] F.L. Lewis, Optimal control, in: W.S. Levine (Ed.), The Control Handbook, CRC Press, Boca Raton, FL, 1996, pp. 759–778.
[10] T. Liu, W. Zhang, F. Gao, Analytical decoupling control strategy using a unity feedback control structure for MIMO processes with time delays, Journal of Process Control 17 (2007) 173–186.
[11] D.E. Seborg, T.F. Edgar, D.A. Mellichamp, Process Dynamics and Control, Wiley, New York, NY, 2004.
[12] Q.-G. Wang, Z. Ye, W.-J. Cai, C.-C. Hang, PID Control for Multivariable Processes, Springer, Berlin (D), 2008.
[13] Q.-C. Zhong, Robust stability analysis of simple systems controlled over communication networks, Automatica 39 (2003) 1309–1312.
[14] Q.-G. Wang, Decoupling with internal stability for unity output feedback system, Automatica 28 (1992) 411–415.
[15] Q.-G. Wang, B. Zou, T.-H. Lee, Q. Bi, Auto-tuning of multivariable PID controllers from decentralized relay feedback, Automatica 33 (1997) 319–330.
[16] K.M. Miettinen, Nonlinear Multiobjective Optimization, Kluwer Academic Publisher, Boston, MA, 1999.
[17] D.M. Prett, C.E. Garcia, Fundamental Process Control, Butterwoths, Stoneham, MA, 1988.
[18] W.L. Luyben, Simple method for tuning SISO controllers in multivariable systems, Industrial and Engineering Chemistry Process Design and Development 25 (1986) 654–660.
[19] D. Semino, C. Scali, Improved identification and autotuning of PI controllers for MIMO processes by relay techniques, Journal of Process Control 8 (3) (1998) 219–227.
[20] Q.-G. Wang, B. Huang, X. Guo, Auto-tuning of TITO decoupling controllers from step tests, ISA Transactions 39 (2000) 407–418.